WAVE LOADS ON RUBBLE MOUND BREAKWATER CROWN WALLS IN LONG WAVES

Mads Sønderstrup Røge[1], Nicole Færch Christensen[1], Jonas Bjerg Thomsen[1], Jørgen Quvang Harck Nørgaard[1], Thomas Lykke Andersen[1]

This paper evaluates the formulae by Nørgaard et al. (2013) for predicting wave loads on rubble mound breakwater crown walls on new model tests. The formulae are tested outside their validation area by means of waves with a low wave steepness and low run-up height compared to the armour freeboard height. Furthermore, both a permeable and an impermeable core are tested. It was found that the formulae by Nørgaard et al. (2013) underestimate the loads for a permeable core and low wave steepness. Therefore, it is recommended that the upper limit for the run-up height by Van der Meer and Stam (1992) is investigated further for different permeabilities. Furthermore, the formulae by Nørgaard et al. (2013) underestimated the wave loads for low relative freeboard heights and it is therefore recommended to make further studies and modify the formulae to also cover these cases.

Keywords: conventional rubble mound breakwater; crown wall; design wave load; long waves

INTRODUCTION

Crown walls are used on breakwaters to provide an access road behind the crown wall and to protect from wave overtopping. The crown wall can be at the same level as the armour crest, or higher to reduce overtopping. Both cases are studied in this paper.

To design a crown wall for stability and internal stresses, the extreme wave loads must be known. Pedersen (1996) adopted the approach by Günbak and Ergin (1983) for run-up and pressure distribution and performed 373 tests in a wave flume to which the formulae were calibrated. The tests were performed with a relative water depth $H_s/h < 0.31$ (i.e. relatively deep water), where H_s is the significant wave height in the time domain and h is the water depth at the toe of the breakwater.

Nørgaard et al. (2013) modified the formula by Pedersen (1996) to include depth-limited conditions ($H_s/h > 0.2$) based on 162 new model tests in a two-dimensional wave flume. These tests were limited to a narrow interval of h/L_{0m} and with deep-water wave steepness $s_{0m} = H_{m0}/L_{0m} > 0.018$, where H_{m0} is the significant wave height in the frequency domain and L_{0m} is the deep water wave length based on the mean wave period T_m. All tests by Nørgaard et al. (2013) and Pedersen (1996) were performed with a permeable core.

This paper presents new model tests with a crown wall on a breakwater with two different permeabilities, a permeable and an impermeable core. The tests mainly focus on waves with a low wave steepness $s_{0m} < 0.01$ often referred to as long waves. The formulae by Nørgaard et al. (2013) are evaluated outside the range of validity of wave conditions and breakwater type, and possible modifications are suggested.

MODEL TEST SET-UP

58 new model tests are performed in a wave flume at Aalborg University, with dimensions 1.5 x 25 x 1 m, cf. Fig. 1. The flume bottom has a slope of 1:100 and thereby the water depth at the wave maker was 0.13 m deeper than at the structure, making it possible to generate depth-limited waves without wave breaking on the paddle.

[1] Department of Civil Engineering, Aalborg University, Sofiendalsvej 9-11, DK-9200 Aalborg SV, Denmark, msr@civil.aau.dk, nicolefaerch@hotmail.com, jbt@civil.aau.dk, jhn@civil.aau.dk, tla@civil.aau.dk

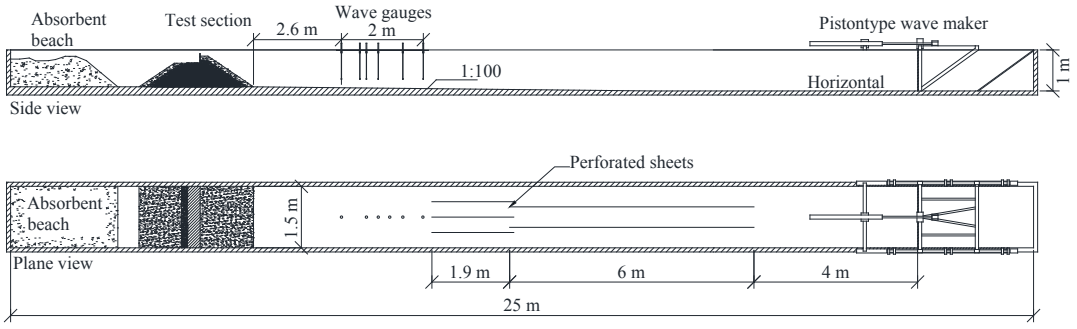

Figure 1: Model set-up of wave flume at Aalborg University.

Four breakwater geometries were tested, a high breakwater for the deep-water conditions $H_{m0}/h \leq 0.2$ and a low for the shallow-water conditions $H_{m0}/h \approx 0.45$ both with a low ($R_{c,low}$) and a high ($R_{c,high}$) wall configuration. The cross sections are illustrated in Fig. 2.

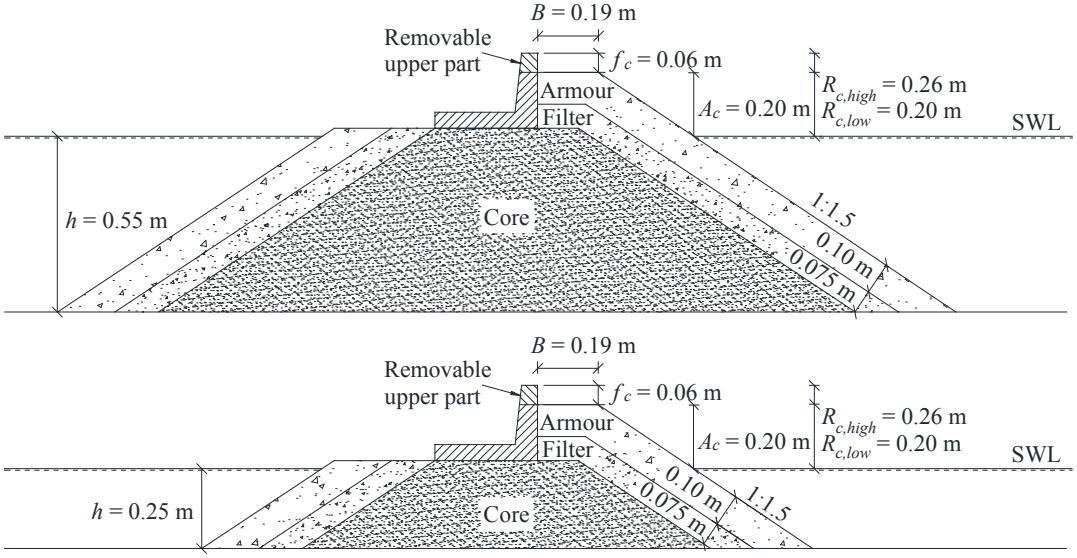

Figure 2: Tested cross sections for shallow-water conditions (bottom) and deep-water conditions (top).

The structures were tested with both an impermeable and a permeable core, making it possible to study the influence of core permeability on the wave loads. The properties of the used materials are shown in Table 1. For the impermeable structure an impermeable membrane was placed between the core and filter layer.

Table 1: Materials used in the cross-sections.

	Core material	Filter material	Armour material
Nominal diameter, $D_{n,50}$ [m]	0.005	0.024	0.042
Mass density, ρ_s [kg/m^3]	3,060	2,615	2,620
Gradation, $f_g = D_{n,85}/D_{n,15}$ [-]	1.60	1.23	1.24

Wave loads were measured by 33 pressure transducers of model series *Drück PMP UNIK* modified to have a flush membrane with a diameter of 20 mm and a correct frequency response up to 5 kHz. The transducers were also used in the tests by Nørgaard et al. (2013). The transducers measured the relative pressure compared to the atmospheric pressure. The influence of temperature and non-linearity was tested and the transducers did not suffer from this. The crown wall was made out of 10 mm thick aluminium plates, fixed to give a stiff structure with high eigen-frequency. The transducers were placed with high density and with overlay to give reliable estimates of the total forces by integration cf. Fig. 3. The crown wall model was constructed with a removable part, making it possible to perform tests with a full protected crown wall or with a protected and unprotected part of the wall.

For horizontal pressures, rows of pressure transducers are used. Presented pressures are the average of the two rows. The procedure of extrapolation and integration of pressures is described later.

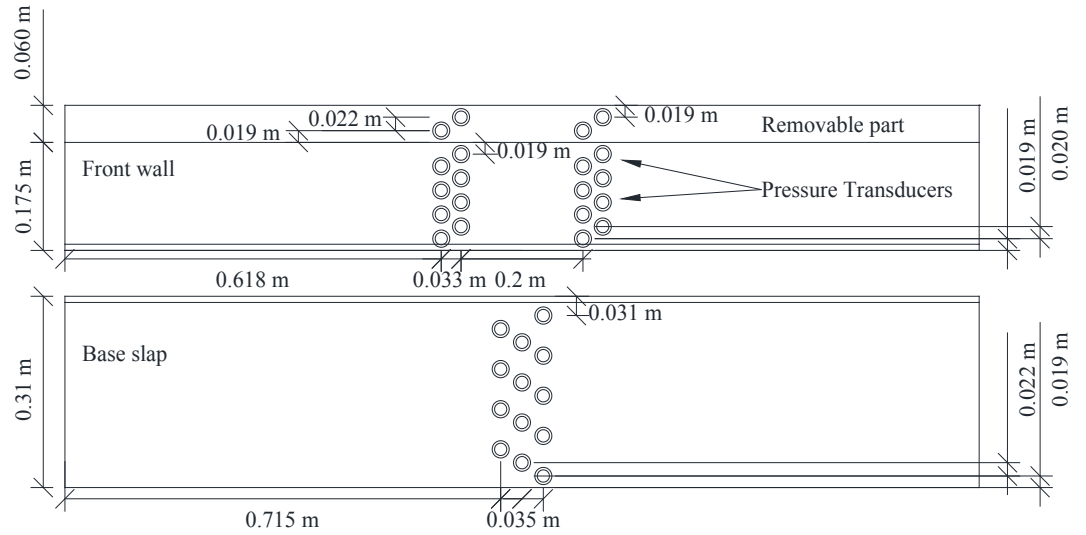

Figure 3: Crown wall with pressure transducers.

WAVE GENERATION AND ANALYSIS

Six wave gauges were placed close to the toe of the structure which made it possible to separate incident waves and reflected waves using the method by Zelt and Skjelbreia (1992). The analysis of the waves were carried out by use of the software package WaveLab 3 (2014). For the frequency domain analysis the surface elevation signals were high- and low-pass filtered at 1/3 f_p and 3 f_p, where f_p is the peak frequency ($1/T_p$). For the time domain analysis no filtering is applied.

The waves were generated from a JONSWAP spectrum using the software package AwaSys 6 (2014). The spectrum is defined by H_{m0}, f_p and the peak enhancement factor γ = 3.3. At least 1,250 waves were generated in each test using a hydraulic driven piston wave maker with active absorption. For the active absorption of the reflected waves, two wave gauges were placed on the face of the wave paddle (see Lykke Andersen et al. (2014)) with an operation area between 0.2 Hz $\leq f \leq$1.2 Hz. For long waves, the system was also effective and showed no standing long waves in the flume. Table 2 shows the tested wave conditions.

Table 2: Tested wave conditions in present study.

H_{m0}/h	s_{0m}	H_{m0}/A_c	h/L_{0m}	ξ_{0m}
0.16-0.45	0.009-0.048	0.39-0.57	0.04-0.27	3.04-6.99

PRESSURE INTEGRATION

Extrapolation and integration of pressures follows the same procedure as Nørgaard et al. (2013). The cross-sectional positioning of transducers is illustrated in Fig. 4 where H_n is horizontal pressures, V_n is

vertical pressures, and h_n and v_n are individual distances between respectively horizontal and vertical pressure points.

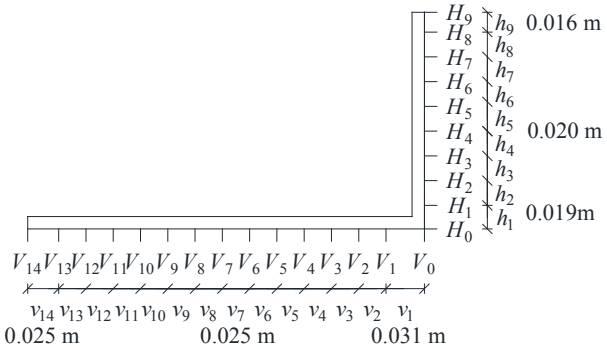

Figure 4: Illustration of pressure points on the crown wall model without the removable part.

V_0, V_{14}, H_0 and H_9 were not measured directly but were determined by a linear extrapolation of neighbouring pressures, cf. Eq. (1), with the restriction of a 0 kPa lower limit.

$$\begin{aligned} H_0 &= H_1 - \frac{H_2 - H_1}{h_2} h_1 \\ H_9 &= H_8 - \frac{H_7 - H_8}{h_8} h_9 \\ V_0 &= H_0 \\ V_{14} &= V_{13} - \frac{V_{12} - V_{13}}{v_{13}} v_{14} \end{aligned} \tag{1}$$

The total horizontal force F_H and the horizontal moment M_{F_H} induced by the waves acting on the crown wall were calculated by linear trapezoidal integration, cf. Eq. (2).

$$\begin{aligned} \Delta F_{H,hn} &= \frac{1}{2} h_n (H_{n\text{-}1} + H_n) \\ F_H &= \sum_{n=1}^{n=9} \Delta F_{H,hn} \\ \Delta M_{F_{H,hn}} &= \frac{1}{2} h_n \left(h_n \left(\frac{1}{3} H_{n\text{-}1} + \frac{2}{3} H_n \right) + (H_{n\text{-}1} + H_n) \sum_{i=1}^{n\text{-}1} h_i \right) \\ M_{F_H} &= \sum_{n=1}^{n=9} \Delta M_{F_{H,hn}} \end{aligned} \tag{2}$$

An example of the pressure distribution and calculated loads for one test, at the time step with maximum horizontal load F_H is shown in Fig. 5.

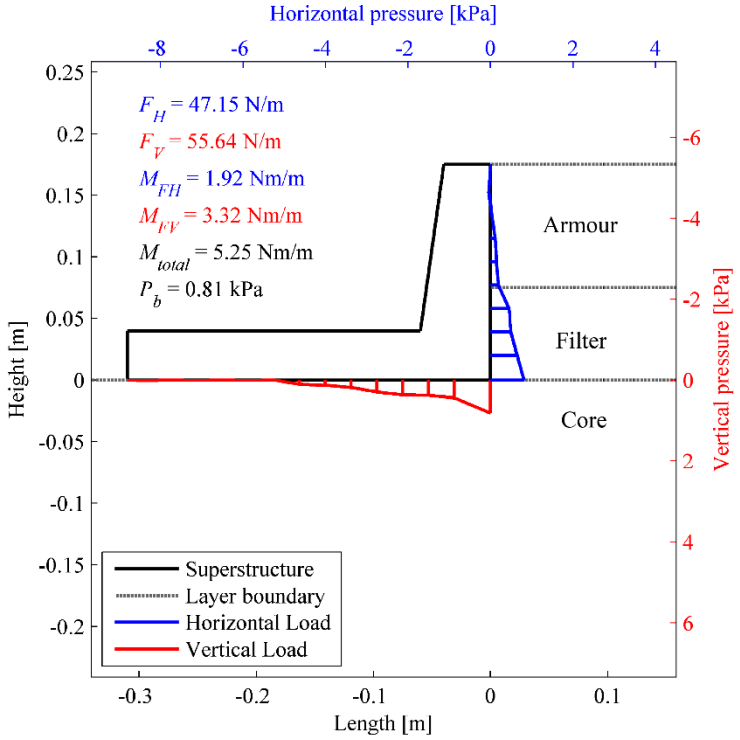

Figure 5: Example of pressure distribution on crown wall for the time step with maximum F_H.

EVALUATION OF WAVE LOAD FORMULA BY NØRGAARD ET AL. (2013)

Formulae by Nørgaard et al. (2013) for prediction of upper and lower wave loads on the un-protected and protected crown wall, F_{Hu}, and F_{Hl}, and the base pressure, P_b, are given in Eq.(3). Fig. 6 illustrates the assumed pressure distribution and the design parameters used in Eq. (3) and (5).

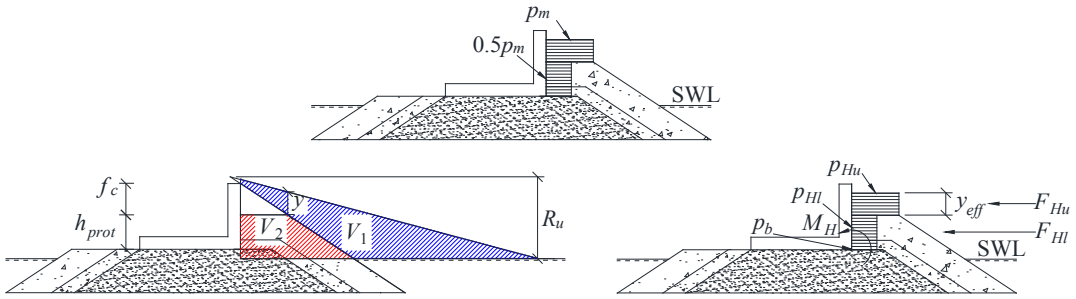

Figure 6: Assumed pressure distribution and definition of design parameters.

Validated ranges of wave conditions and structure dimensions by Nørgaard et al. (2013) are presented in Table 3.

Table 3: Validated ranges by Nørgaard et al. (2013) formula.

Parameters	Ranges $f_c = 0$	Ranges $f_c > 0$
ξ_{0m}	2.30-4.90	3.31-4.64
H_s/A_c	0.50-1.63	0.52-1.14
R_c/A_c	0.78-1	1-1.70
A_c/B	0.58-1.21	0.58-1.21
H_{m0}/h	0.19-0.55	0.19-0.55
s_{0m}	0.018-0.073	0.02-0.041
h/L_{0m}	0.06-0.10	0.06-0.066

$$
\begin{aligned}
y_{eff} &= \min\left(\frac{y}{2}\,;f_c\right)\\
F_{Hu,0.1\%} &= a\sqrt{\frac{L_{0m}}{B}}\,p_m\,y_{eff}\,b\\
F_{Hl,0.1\%} &= \frac{1}{2}\,a\sqrt{\frac{L_{0m}}{B}}\,p_m\,V\,b\\
p_m &= g\,\rho_w\max\left(R_{u,0.1\%}-A_c;0\right)\\
P_{b,0.1\%} &= d\,V\,p_m\\
V &= \begin{cases}\frac{V_2}{V_1} & \text{for} \quad V_2 < V_1\\ 1 & \text{for} \quad V_2 \geq V_1\end{cases}
\end{aligned}
\tag{3}
$$

Where $a = 0.21$, $b = 1$ and $d = 1$ are empirical factors, T_m is the mean zero down crossing period, $L_{0m} = g\,T_m^2/(2\pi)$ is the deep-water wave length, ρ_w is the mass density of water, p_m is the stagnation pressure, $R_{u,0.1\%}$ is the run-up height exceeded by 0.1% of the incident waves and $H_{0.1\%}$ is the wave height exceeded by 0.1% of the waves.

Nørgaard et al. (2013) suggested to couple $R_{u,0.1\%}$ to $H_{0.1\%}$ to include depth-limited conditions for the run-up formula by Van der Meer and Stam (1992). The modified run-up formula by Nørgaard et al. (2013) is stated in Eq. (4).

$$
\begin{aligned}
R_{u,0.1\%} &= \begin{cases}0.603\,H_{0.1\%}\,\xi_{0m}, & \xi_{0m} \leq 0\\ 0.722\,H_{0.1\%}\,\xi_{0m}^{0.55}, & \xi_{0m} > 0\end{cases}\\
R_{u,0.1\%} &\leq 2.58\,H_s \text{ for permeable slopes}\\
\xi_{0m} &= \frac{\tan\alpha}{\sqrt{\frac{2\pi}{g}\,\frac{H_{m0}}{T_m^2}}}
\end{aligned}
\tag{4}
$$

Nørgaard et al. (2013) modified the formula for the overturning moment by dividing it in two parts, the lower and upper part of the horizontal load.

$$
\begin{aligned}
F_{H,0.1\%} &= F_{Hu,0.1\%} + F_{Hl,0.1\%}\\
M_{H,0.1\%} &= \left(h_{prot}+\frac{1}{2}\,y_{eff}\,e_2\right)\,F_{Hu,0.1\%}+\frac{1}{2}\,h_{prot}\,F_{Hl,0.1\%}\,e_1
\end{aligned}
\tag{5}
$$

Where $e_1 = 0.95$ and $e_2 = 0.4$ are empirical factors.

Permeable Core

Fig. 7 shows that most of the data within the validation area (filled markers) are inside the 90% confidence band. Outside the validation area (open markers) the present tests provided mainly higher loads than predicted by the formulae by Nørgaard et al. (2013).

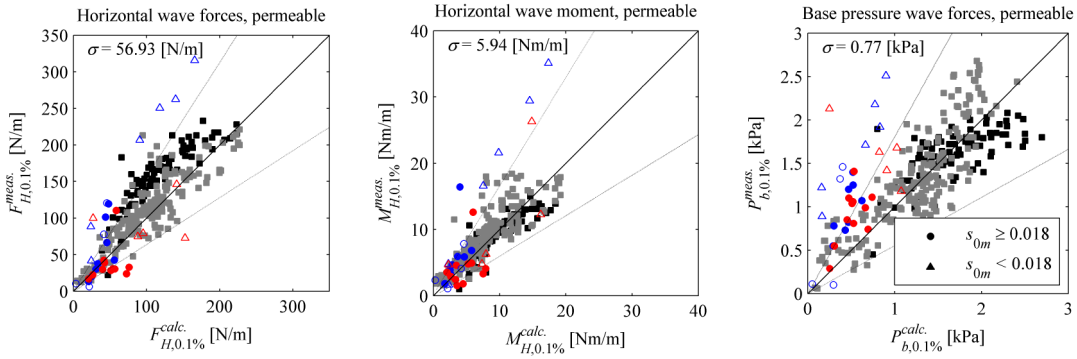

Figure 7: Comparison between measured and calculated values. The blue markers are for deep-water conditions and red is for shallow-water conditions. The open markers illustrate the tests which are outside the validation area of Nørgaard et al. (2013). The grey markers are Nørgaard et al. (2013) data and the black markers are Pedersen (1996) data. The standard deviations σ are the differences between measured and calculated loads for the present data. The grey lines are the 90% confidence band.

Two effects are expected to affect the underestimations of wave loads by Nørgaard et al. (2013). First reason could be that the stagnation pressure p_m in Eq. (3) predicts no loads when the run-up height $R_{u,0.1\%}$ is equal or lower than the armour freeboard height A_c. This is described later for the impermeable core. The second reason could be the influence of the upper limit in the run-up formula (Eq. (4)), which can be seen in Fig. 7 as underestimated results are present for $s_{0m} < 0.018$. The formulae by Nørgaard et al. (2013) are neglecting the quasistatic pressure which may be another reason for underestimation of the loads, especially for $s_{0m} < 0.018$.

Upper Limit for Run-up Height

The run-up heights were not measured during the tests, but it was observed from video that the run-up height exceeded the upper limit given in Eq. (4). Fig. 8 shows that the calculated run-up height is lower than the actual run-up height. The calculated $R_{u,0.1\%}$ is based on a breakwater with no overtopping which is not the case in Fig. 8 since the water hits the crown wall, and therefore the actual run-up height must be higher than observed. The upper limit for the run-up height is given by the permeability; permeable or impermeable, which might be too coarse a division.

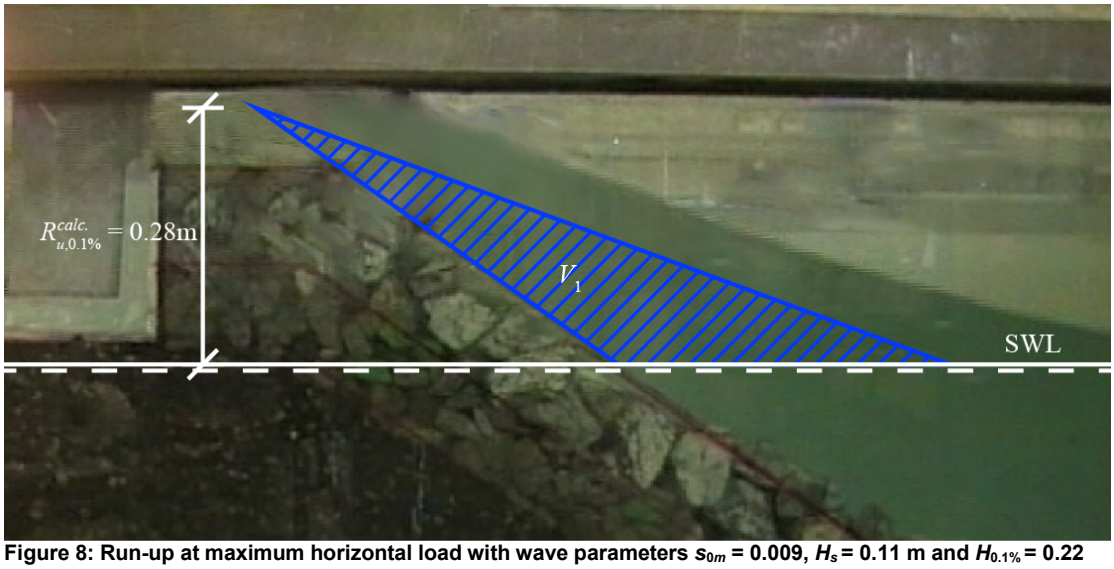

Figure 8: Run-up at maximum horizontal load with wave parameters s_{0m} = 0.009, H_s = 0.11 m and $H_{0.1\%}$ = 0.22 m.

When increasing the upper limit in Eq. (4) the long waves will get a larger run-up height and thereby larger predicted loads. Fig. 9 shows the results of the best fit of the upper limit to the present data, where the original limit $R_{u,0.1\%} = 2.58\ H_s$ is changed to $R_{u,0.1\%} = 3.03\ H_s$ as an initial estimate. Further tests are needed to determine the exact upper limit of the run-up height related to the degree of permeability for

the structure and other relevant parameters. The improvement to the calculated loads when correcting the upper limit is seen when comparing Fig. 7 with Fig. 9 for $s_{0m} < 0.018$.

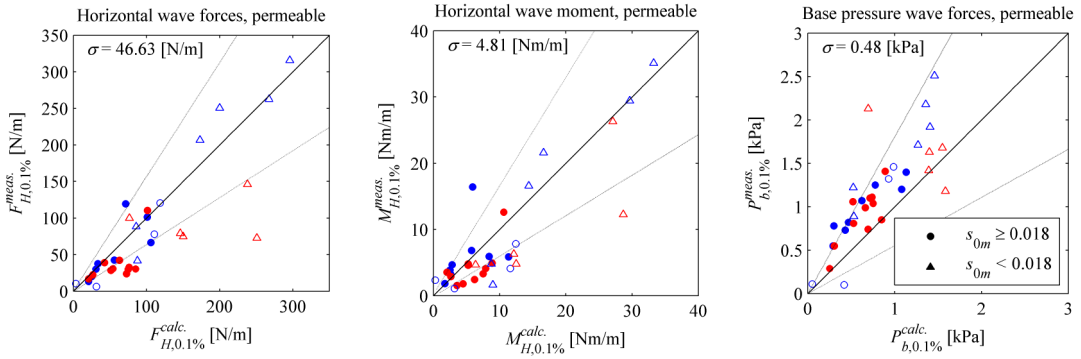

Figure 9: Comparison between measured and calculated values for the permeable core with adjusted upper limit. The blue markers are for deep-water conditions and red is for shallow-water conditions. The standard deviations *σ* are the differences between measured and calculated loads for the present data. The grey lines are the 90% confidence band.

Fig. 9 shows that values $F_{H,0.1\%}$ and $M_{H,0.1\%}$ on shallow-water waves and for low steepness waves ($s_{0m} < 0.018$) are slightly overestimated. The reason for this can be a poor prediction of the run-up height which is investigated in an ongoing study or due to not considering reflection and impulsive peaks separately.

The modification made the prediction significantly better for the long waves. The upper limit of the run-up height should be used with caution since it can give unsafe results if set too low, and conservative results if set too high. Further investigation is therefore needed to get a better estimation of the run-up height for the long waves and for permeable structures.

Impermeable core

There is no upper limit for the run-up height for impermeable cores (cf. Eq. (4)). Nørgaard et al. (2013) overestimate slightly the loads for the impermeable core as shown in Fig. 10, however, most markers are within the confidence band.

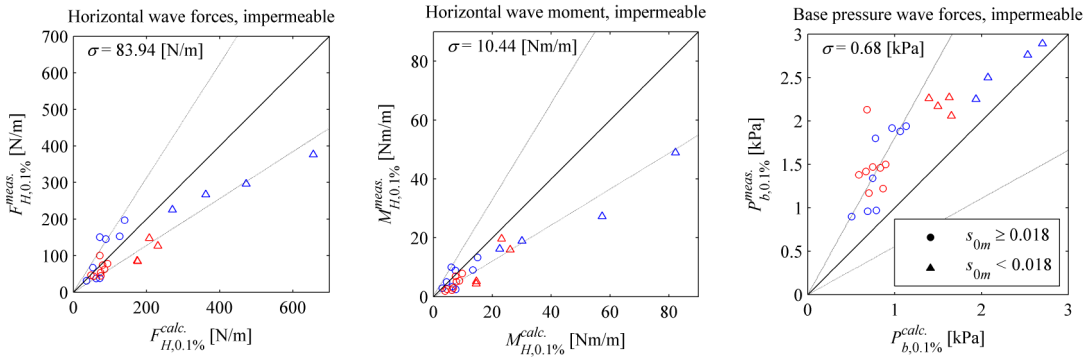

Figure 10: Comparison between measured and calculated values for the impermeable core. The blue markers are for deep-water conditions and red markers are for shallow-water conditions. The standard deviations *σ* are the differences between measured and calculated loads for the present data. The grey lines are the 90% confidence band.

However, the base pressure ($P_{b,0.1\%}$) has an significantly unsafe bias. The reason for this could be that the run-up height is very close to the freeboard height in some of the tests which leads to an underestimation of the base pressure. The prediction error for the impermeable core compared to ($R_{u,0.1\%}$ - A_c)/H_s is illustrated in Fig. 11.

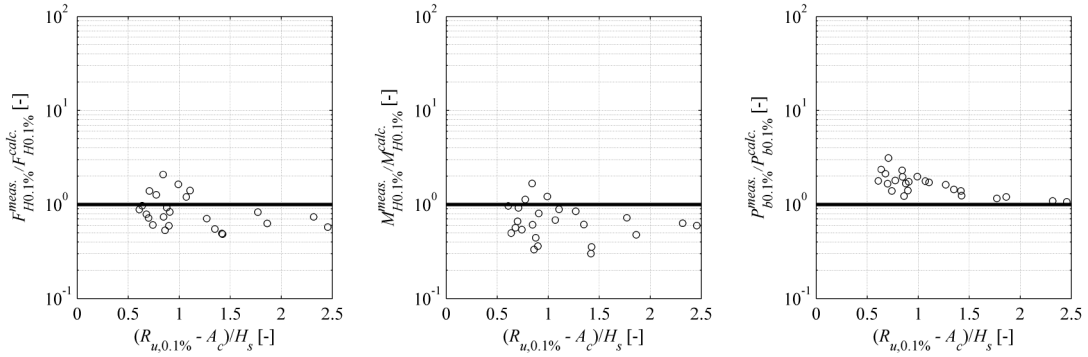

Figure 11: Prediction error compared to the run-up height and freeboard for the impermeable core.

From Fig. 11 it is clear that the prediction error of the base pressure ($P_{b,0.1\%}$) is larger when ($R_{u,0.1\%}$ - A_c)/H_s approach zero.

The run-up height is an important parameter in the prediction of the loads on a crown wall. Therefore, other run-up formulae could be tested (e.g. EurOtop (2007) where the influence of the roughness, berm and oblique waves are included). This has not been tested further in the present study.

CONCLUSION

In this paper it has been shown that for a permeable core the formula by Nørgaard et al. (2013) overestimates forces on the crown when exposed to long waves. The calculated base pressure is zero for run-up heights lower than the freeboard height, which was not the case in the present test. No changes to the formulae were proposed to correct the error for low run-up heights compared to the freeboard, but changes to the prediction of the stagnation pressure are investigated in an ongoing study. For deep-water conditions and the permeable core, the prediction error for long waves could be corrected by changing the upper limit for the run-up formula.

The loads for the impermeable core on deep-water were slightly overestimated when using the formulae by Nørgaard et al. (2013) although most markers are within the confidence band. The formulae deviated for low run-up heights compared to the armour freeboard height.

REFERENCES

AwaSys 6. 2014. Wave Generation Software, Department of Civil Engineering, Aalborg University, http://www.hydrosoft.civil.aau.dk/awasys/.

EurOtop Manual. 2007. Overtopping Manual; Wave Overtopping of Sea Defences and Related Structures – Assessment Manual. UK: N.W.H. Allsop, T. Pullen, T. Bruce. NL: J.W. van der Meer. DE: Schüttrumpf, H., Kortenhaus, A. www.overtopping-manual.com.

Günback, A.R. and Ergin, A. 1983. Damage and repair of Antalya harbor breakwater. Proc. Conf. on Coastal Structures, Alexandria, Egypt.

Lykke Andersen, T., Clavero, M., Frigaard, P., Losada, M., Puyol, J.I. 2014. Active Absorption of highly non-linear waves. Submitted to Coastal Engineering for review.

Nørgaard, J.Q.H., Andersen, T.L., Burcharth, H.F. 2013. Wave loads on rubble mound breakwater crown walls in deep and shallow water wave conditions. Coastal Engineering, 80, pp. 137-147.

Pedersen, J. 1996. Wave Forces and Overtopping on Crown Walls of Rubble Mound Breakwaters. Ph.d. thesis, Series paper 12, ISBN 0909-4296, Hydraulics & Coastal Engineering Lab., Dept. of Civil Engineering, Aalborg University, Denmark.

Van der Meer, J.W., Stam, C.J.M. 1992. Wave run-up on smooth and rock slopes. ASCE, Journal of WPC and OE 188 (No. 5), 534–550 (New York. Also Delft Hydraulics Publication No. 454).

WaveLab 3. 2014. Wave Data Acquisition and Analysis Software, Department of Civil Engineering, Aalborg University, http://www.hydrosoft.civil.aau.dk/wavelab/.

Zelt, J. A. and Skjelbreia, J. E. 1992. Estimating incident and reflected wave fields using an arbitrary number of wave gauges. Coastal Engineering Proceedings, 1(23).